

Article

Extending the NNO Ballistic Limit Equation to Foam-Filled Dual-Wall Systems

William P. Schonberg

Civil Engineering Department, Missouri University of Science & Technology, Rolla, MO 65409, USA; wschon@mst.edu

Abstract: A key component in the quantitative assessment of the risk posed to spacecraft by the micrometeoroid and orbital debris (MMOD) environment is frequently referred to as a ballistic limit equation (BLE). A frequently used BLE for dual-wall configurations (which are commonly used on spacecraft to protect them against the MMOD environment) is the New Non-Optimum, or “NNO”, BLE. In design applications where a BLE is needed for a new structural system that has not yet been tested, but resembles to a fair degree a dual-wall system, it is common practice to equivalence the materials, thicknesses, etc., of the new system to the materials, thicknesses, etc., of a dual-wall system. In this manner, the NNO BLE can be used to estimate the failure / non-failure response characteristics for the new system. One such structural wall system for which a BLE does not yet exist is a dual-wall system that is stuffed with a lightweight polymer-based foam material. In this paper we demonstrate that the NNO BLE, in its original form, frequently over- or under-predicts the response of such a system. However, when the NNO BLE is modified to more properly include the effects of the presence of the foam as well as the actual material properties of the walls and the impacting projectile, there is a marked improvement in its predictive abilities.

Keywords: ballistic limit equation; dual-wall system; foam-filled; hypervelocity impact; space debris



Citation: Schonberg, W.P. Extending the NNO Ballistic Limit Equation to Foam-Filled Dual-Wall Systems. *Appl. Sci.* **2023**, *13*, 800. <https://doi.org/10.3390/app13020800>

Academic Editors: Lorenzo Olivieri, Kanjuro Makihara and Leonardo Barilaro

Received: 15 November 2022

Revised: 28 December 2022

Accepted: 29 December 2022

Published: 6 January 2023



Copyright: © 2023 by the author. Licensee MDPI, Basel, Switzerland. This article is an open access article distributed under the terms and conditions of the Creative Commons Attribution (CC BY) license (<https://creativecommons.org/licenses/by/4.0/>).

1. Introduction

A key component in a probabilistic risk assessment for spacecraft being designed to operate in the micrometeoroid and orbital debris (MMOD) environment is a ballistic limit equation, or BLE. This is an equation used to determine if a spacecraft component will suffer a critical failure following an on-orbit high-speed impact.

One type of BLE is derived from a damage predictor equation that is itself obtained from a curve-fit of a damage measurements, such as crater depth or hole diameter, in terms of impact parameters, material properties, and target configuration. The other kind of BLE is basically a “hand-drawn” discriminant line that, for example, separates (projectile diameter, impact velocity) combinations that cause failure from those that do not. It is these types of BLEs that were used to design the MMOD shielding on the International Space Station (see, e.g., [1] for more information on how such BLEs were developed).

A frequently used BLE for dual-wall configurations (also known as “Whipple Shields”) is the New Non-Optimum, or NNO, BLE [2]. These wall designs are frequently used on spacecraft to protect them against the threats posed by MMOD particles impacts. The NNO BLE consists of three parts in terms of increasing impact velocity—a low velocity portion (through approx. 3 km/s), a high velocity portion (above approx. 7 km/s), and a linear interpolation between the BLE values at the end of and the start of the low and high velocity portions, respectively.

Quite frequently, a BLE is needed for a new structural system or element that has not yet been tested, but resembles to a fair degree a dual-wall system for which the NNO BLE would be applicable. In such cases it is common practice to equivalence the materials, thicknesses, etc., of the system or element of interest (but for which a BLE does not yet

exist) to the materials, thicknesses, etc., of a dual-wall system. In this manner, the NNO BLE can be used to estimate the failure/non-failure response characteristics for the new system of interest without having to expend significant resources to generate a BLE for that new system.

One such structural wall system for which a BLE does not yet exist, but is also seeing an increase in application, is a dual-wall system that is completely filled with a lightweight foam material (i.e., there are no discernable air gaps between either wall of the dual-wall system and the foam filling the space between them). The outer and inner walls in such a system could be aluminum, or made out of a composite material. Since such a system bears a close resemblance to a more standard dual-wall system (where the space between the outer and inner walls is empty), it could be considered appropriate to re-cast the foam-stuffed dual-wall system as an “empty” all-aluminum Whipple Shield with wall thicknesses that take into account any non-aluminum wall materials as well as the presence of the foam stuffing in the original system.

In such a dual-wall configuration, the foam between the outer and inner walls can be either metallic (e.g., lightweight aluminum foams), or non-metallic (e.g., lightweight polymer foams like polyurethane). The focus of the study described herein was on lightweight non-metallic polymer-based foams. Even then, the space between the outer and inner walls could be either fully filled or partially filled. We again focus our attention on dual-wall systems that are fully filled with foam. In this manner, the foam in the configuration we studied not only could affect the protective capability of the dual-wall system, but it also would provide some structural support to keep the outer wall at a constant distance away from the inner wall. This is especially important in applications where the outer and inner walls might be made of extremely flexible materials, such as composite fabrics or very thin metallic plates.

As will be seen shortly, we found that the NNO BLE in its original form frequently over- or under-predicted the response of such a system. However, when the NNO BLE was modified to more properly include the effects of the presence of the stuffing as well as the actual material properties of the walls and the impacting projectile, we found that there was a marked improvement in its predictive abilities.

In this paper, then, we present the results of a study whose goal was to improve the predictive ability of the NNO BLE when it is applied to the particular dual-wall construction involving metallic or non-metallic outer and inner walls, the space between which is filled with a non-metallic lightweight foam. In this study, we developed a set of functions that, when incorporated into the NNO BLE, does significantly improve its predictive ability for this type of wall system. This is demonstrated by comparing the predictions of the original and modified versions of the NNO BLE against experimental data and the results of hydrocode simulations for a variety of wall materials, foam materials, and projectile materials, and for impact velocities ranging from approx. 2–40 km/s.

2. Impact Conditions and Dual-Wall Constructions

A sketch of the target is shown in Figure 1—it consists of outer and inner walls (which could be either metallic or non-metallic) separated from each other by a small gap that is filled with a lightweight (or low density) non-metallic foam.

The Dual-wall Configuration



Figure 1. Sketch of a Dual-Wall Configuration Stuffed with Light-weight Foam.

Tables 1–3 below present a summary of the impact parameters, configurations, and material properties of the dual-wall targets used in the experimental test programs and numerical simulations that generated the data used in this study. Projectile density values in Table 1 were found, for the most part, in the reports or articles summarizing the test programs wherein those projectiles were used; others, where values were not provided, were obtained from an online database [3]. Additionally, the “diameters” of the disk projectiles are actually the equivalent spherical projectile diameters calculated using an equal-mass consideration.

Table 1. Impact Conditions in Previous Experimental Programs and Numerical Simulations.

Ref #	Projectile Shape	Projectile Material	Proj Mat'l Density (gm/cm ³)	Proj Diam (mm)	Impact Velocity (km/s)	Impact Obliquity (deg)
[4]	Sphere	Pyrex	2.12	1.60	5.8–6.5	0
[5]	Disk	MgLi	1.35	0.909	5.0–5.5	0
[6]	Sphere	Aluminum	2.80	6.35	5.0–6.0	0
[6]	Disk	Lexan	1.20	6.60, 7.27	4.5–8.2	0
[7]	Disk	PETP ¹	1.38	2.49	2.0–5.8	0
[8–11]	Sphere	Al 2017-T4	2.80	1.9–7.0	6.8–7.1	0, 30, 60
[12]	Sphere	Al 2017-T4	2.80	0.8–2.1	7, 25	30

¹ PETP ... polyethylene terephthalate.

Table 2. Target Configurations and Materials Used in Previous Experimental Programs and Numerical Simulations.

Ref #	Outer Wall Material	Outer Wall Thick (cm)	Filler Material	Filler Material Density (gm/cm ³)	Filler Material Thick (cm)	Inner Wall Material	Inner Wall Thick (cm)
[4]	Al 2024-T3	0.030–0.056	Polyurethane	0.005–0.102	5.08, 7.62	Al 2024-T3	0.030–0.056
[5]	Al 2024-T3	0.0076	Polyurethane, Styrofoam	0.0285, 0.0288	0.483	Al 2024-T3	0.0127, 0.0254
[6]	Al 2024-T3	0.0508	Polyurethane	0.0320, 0.0336	3.81	Al 2024-T3	0.127
[7]	PETP ¹ Fabric	0.127	Polyurethane	0.0230	3.94–4.32	PETP ¹ (Coated and Uncoated)	0.063–0.127
[7]	Laminated and Unlaminated Rayon Fabric	0.064, 0.089	Polyurethane	0.0208	3.81–4.18	Rayon Fabric	0.071
[8–10]	Al 6061-T6	0.05	Polyimide	0.0056	2.0	Al 6061-T6	0.05
[11]	T300/Epoxy	0.097	Polymethacrylimide	0.0521	2.35	T300/Epoxy	0.097
[12]	Al 6061-T6	0.05	Polyimide	0.0056	2.0	Al 6061-T6	0.05
[12]	Glass/Epoxy	0.05	Polyimide	0.0056	5.0	IM7/Epoxy	0.101

¹ PETP ... polyethylene terephthalate.

Filler material density values in Table 2 are, except for Refs. [8–12], as specified in the reports or articles summarizing the test programs wherein those materials were used; density values for polyimide and polymethacrylimide were also obtained from the same online database [3]. Likewise, in Table 3, outer and inner wall density values are also, for the most part, as specified in the various referenced reports or articles; density values not

provided in the test program references were either obtained from the online database [3], or calculated using other information given elsewhere in the referenced documents. Outer and inner wall strength values were typically not provided in the reference documents, and so were estimated using strength values for similar materials provided elsewhere as indicated.

Table 3. Density and Strength Values for Inner Wall Materials.

Wall Type	Material	Density (gm/cm ³)	Source	Strength (ksi)	Source
Outer Wall	PETP Fabric	0.769	Values as specified in references where used matweb.com	Outer wall strength values not required for NNO BLE	
	Rayon Fabric	0.713 ¹ , 0.474 ²			
	T300/Epoxy	1.53			
	Glass/Epoxy	1.90			
Inner Wall	PETP Fabric	0.953 ³ , 0.832 ⁴	Values as specified in references where used	56.8	Ref. [13]
	Rayon Fabric	0.549		60.0	Ref. [14]
	T300/Epoxy	1.53, 1.64		290, 264	Toray data sheets
	IM7/Epoxy	1.58		397	Hexcel data sheets

¹ Laminated Fabric, ² Unlaminated fabric, ³ Elastomer coated fabric, ⁴ Uncoated fabric.

3. Modifications to the NNO BLE

In this study we developed a set of functions that, when incorporated into the NNO BLE, significantly improve its predictive ability for a foam-filled dual-wall system. These functions were intended to more properly take into account the material properties of the impacting projectile and the walls in the dual-wall system. In the modified NNO BLE, the presence of the foam in the dual-wall system under consideration is taken into account in the same manner in which they are traditionally included when the original NNO BLE is applied to such dual-wall systems. Namely, in both cases, the thicknesses of the outer and inner walls are increased slightly using a mass equivalence calculation that allocated 50% of the foam filler mass to the outer wall and 50% to the inner wall.

The following equation gives a top-level perspective of how the original NNO BLE is to be modified for these types of wall configurations:

$$d_{crit}^{mod} = d_{crit}^{orig} * f_1(\rho_{rw}, \sigma_{rw}) * f_2(\rho_p) * f_3(\theta_p) \tag{1}$$

where d_{crit}^{mod} and d_{crit}^{orig} are the modified and original critical, or ballistic limit, projectile diameters as predicted by the modified and original NNO BLE, respectively. In this equation, the function f_1 accounts for the inner wall density and strength, if different from aluminum, the function f_2 accounts for the density of non-aluminum projectiles, and the function f_3 accounts for the effects of impact obliquity.

The forms of the modifier functions $f_1, f_2,$ and f_3 in Equation (1) are guided by expected asymptotic function values or the roles played by those functions in modifying the original NNO BLE. For example, as projectile density approaches that of aluminum (from below, that is, when ρ_p becomes greater than ~ 2.0 gm/cm³), all modification functions should approach unity (i.e., the modifiers should all approach unity when aluminum projectiles are considered because that is the projectile material on which—for the most part—the NNO BLE is based). The same should be true when aluminum walls are used, that is, when ρ_{rw} and σ_{rw} take on values corresponding to those of aluminum—in these cases, the values of the modifier functions should then also all approach unity. The following equations define the modifying functions $f_1, f_2,$ and f_3 :

$$f_1(\rho_{rw}, \sigma_{rw}) = 1 - \exp\left\{-15.73 \left[(f_{RWS} * f_{RWD})^{-9.826} \right] \right\} \tag{2}$$

where

$$f_{RWS} = (\sigma_{RW} / 50)^{\{1 - \exp[-7.158(\sigma_{RW} / 50)^{-3.949}]\}} \tag{3a}$$

$$f_{RWD} = (\rho_{RW}/2.71)^{\{3.0[1-\exp(-0.007967\rho_{RW}^{12.34})]\}} \tag{3b}$$

$$f_2(\rho_p) = 1 + (MF_0 - 1) * \left[1 - \exp\left(-f_{PD}(1 - V_P/72)^{f_{VP}}\right) \right] / [1 - \exp(-f_{PD})] \tag{4}$$

with

$$\left\{ \begin{matrix} MF_0 \\ f_{PD} \\ f_{VP} \end{matrix} \right\} = 1 + (A - 1) \left\{ 1 - \exp\left[-B(1 - \rho_P/10.0)^C\right] \right\} / [1 - \exp(-B)] \tag{5}$$

where the constants *A*, *B*, and *C* are given for each equation in Table 4 below, and

$$f_3(\theta_p) = 1 + 0.075V_P^{0.9033}\theta_p^{0.2084} \tag{6}$$

In Equations (2), (3) and (6), constants and coefficients with 4 significant figures were obtained through curve-fitting exercises using the desired functional forms. As noted previously, these functional forms were informed by desired function values as inner wall material property values approached certain values within the impact test database used in this study.

Alternatively, the constants 50, 2.71, and 72 (and the 2.85 in Equation (5) as well) were used to, in effect, non-dimensionalize corresponding numerators to render the terms within the desired functions to have values of similar orders of magnitude. This, in turn, facilitated the regression exercise that yielded the other constants in the various functions.

Finally, the values of the constants *A*, *B*, and *C* in Equations (4) and (5), that is, those in Table 3, were obtained manually using two considerations. First, the function values had to approach expected asymptotic values, and second, the correctness of the BLE predictions was maximized to the highest extent possible. That is, BLE predictions of ballistic limit diameter were checked to ensure that they were, as often as possible, (1) larger than actual projectile diameters in tests where the inner walls were not perforated, and (2) smaller than actual projectile diameters when inner walls were perforated.

Table 4. Parameter Values for Lower Projectile Density Function.

	A	B	C
<i>MF</i> ₀	3.0	1.4 × 10 ³	45
<i>f</i> _{PD}	2.4 × 10 ³	2.0 × 10 ⁹	163
<i>f</i> _{VP}	100.0	3.4 × 10 ⁴	70

In these equations, the various input parameters are defined as follows:

*ρ*_P is the projectile material density (in gm/cm³)

*ρ*_{RW} is the inner wall material density (in gm/cm³)

*σ*_{RW} is the inner wall material tensile strength (in ksi)

*θ*_P is the trajectory obliquity (radians)

*V*_P is the impact velocity (km/s)

4. Comparison with Test Data and Numerical Simulation Predictions

The next series of plots shows comparisons between the predictions of the original NNO BLE and NNO BLE as modified according to Equations (1)–(4). Two types of plots were used for comparison for different configurations:

- *D*_{proj}/*D*_{crit} vs. *V*_{imp}—When the ratio > 1, did the test result in an inner wall perforation for that particular impact velocity? Likewise, when the ratio < 1, did the test result in a non-perforation event?

- D_{crit} vs. V_{imp} —Are the tests with the inner wall perforations above the ballistic limit curve, and are those without inner wall perforation below the curve, as impact velocity is increased?

In these plots, the original NNO BLE predictions of D_{crit} are calculated with the following parameter modifications as necessary:

- *Projectile Density*—density of actual projectile material
- *Outer Wall Thickness*—mass equivalent aluminum thickness (assuming an aluminum density of 2.71 gm/cm^3) for original outer wall material and thickness and 50% of the foam stuffing
- *Outer Wall Density*—density of original aluminum outer wall material, or 2.71 gm/cm^3 if mass equivalent aluminum outer thickness is being used
- *Stand-off Distance or Spacing*—this is the thickness of the foam between the outer wall and the inner wall
- *Inner Wall Thickness*—mass equivalent aluminum thickness (assuming an aluminum density of 2.71 gm/cm^3) for original inner wall material and thickness and 50% of the foam stuffing
- *Inner Wall Density*—density of original aluminum inner wall material, or 2.71 gm/cm^3 if mass equivalent aluminum bumper thickness is being used
- *Inner Wall Yield Strength*—actual yield strength for aluminum inner wall materials; ultimate tensile strength for non-aluminum inner wall materials

Figures 2–4 show a comparison between the plots of the modified and original NNO BLEs for several different constructions of polyurethane-filled dual-wall systems impacted by non-aluminum projectiles. Additionally, shown are the experimental results from [6,8] regarding whether or not the inner walls of the dual-wall systems were perforated (P) or not (NP). In Figure 2, the original and modified BLEs shown were obtained using inner wall density, inner wall thickness, and filler thickness parameter values averaged across the various dual-wall constructions in [8].

It is evident from these plots that the original formulation of the NNO BLE, as implemented above, did not adequately model the P/NP response of those particular foam-filled dual-wall systems. That is, while most of the tests with the inner wall perforations (the hollow P datapoints) were above the original NNO ballistic limit curves as expected, those without inner wall perforation (the solid NP datapoints) were not below the original NNO BLE curves. However, when the modifications to the original NNO BLE were implemented as described above, the hollow P datapoints (for the most part) remained above the modified NNO ballistic limit curves, while the solid NP datapoints were now (for the most part) below the modified NNO BLE curves.

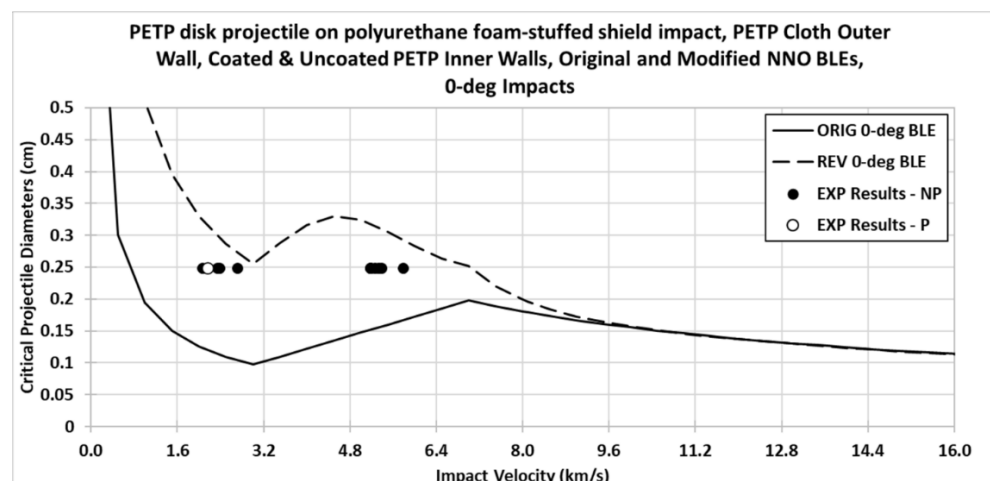


Figure 2. Comparison of Original and Modified NNO BLEs against P/NP data in [8] for Dual-Wall Systems with PETP Outer Walls and PETP Inner Walls.

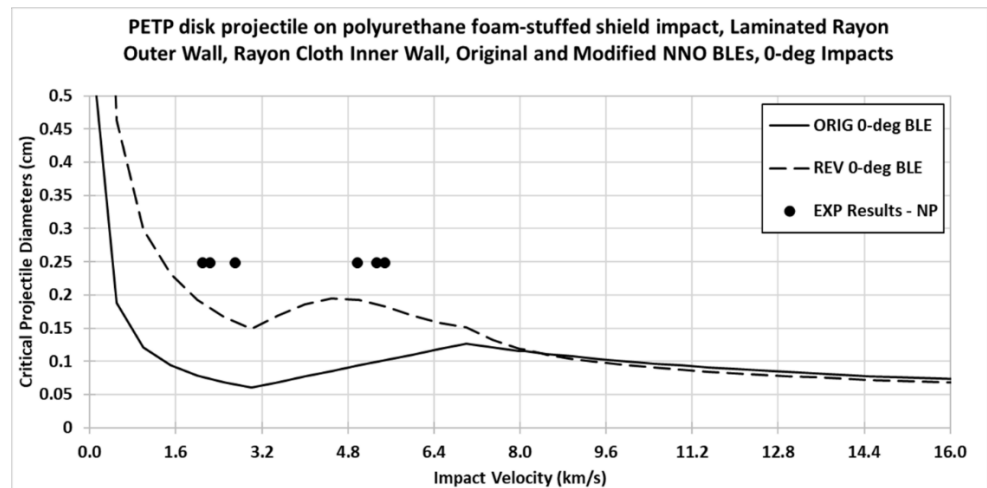


Figure 3. Comparison of Original and Modified NNO BLEs against P/NP data in [8] for Dual-Wall Systems with Rayon Outer and Inner Walls.

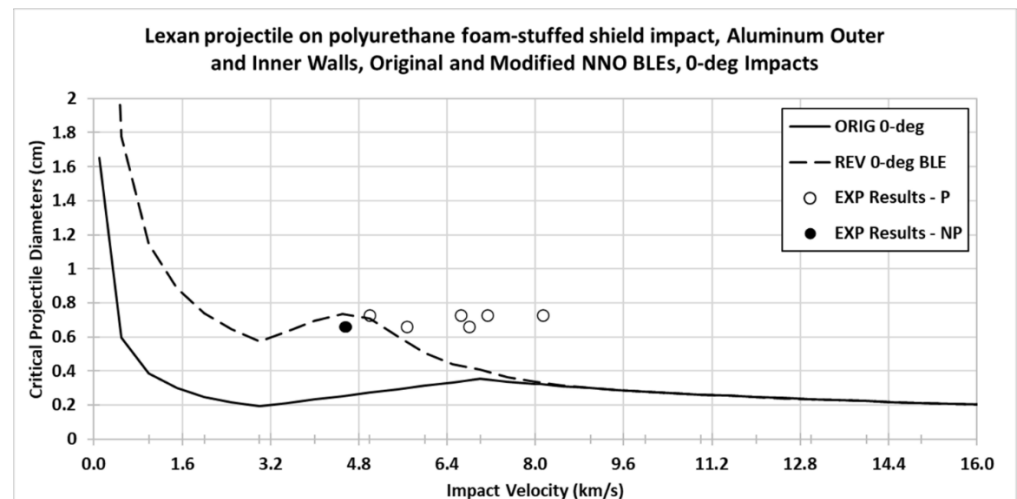


Figure 4. Comparison of Original and Modified NNO BLEs against P/NP data in [6] for Dual-Wall Systems with Aluminum Outer and Inner Walls.

This change is a significant improvement in the ability of the (modified) NNO BLE to predict the P/NP response of foam-filled dual-wall systems with aluminum as well as composite material outer and inner walls (at least for impact velocities between 2 and 8 km/s). Of course, as can be seen in Figure 3, the modified NNO BLE, while significantly closer to the NP datapoints than the original NNO BLE, failed to end up above those points. So while an accuracy improvement is still evident for the modified NNO BLE over the original NNO BLE for foam-filled dual-wall systems with laminated rayon outer walls and cloth or fabric inner walls, there are still some response characteristics not entirely correctly captured by the modifications made to the original NNO BLE for this particular dual-wall configuration.

In Figure 2, we also see that while all of the non-perforation datapoints are now below the modified NNO BLE, the perforation datapoint is not above it, as it should be. Of additional interest is that it appears to fall amidst a series of non-perforation datapoints, indicating that there might be something amiss with this test that resulted in a perforation. However, all of the datapoints in Figure 4 do appear to fall on the correct sides of the modified NNO BLE—the non-perforation datapoint is below it, and all of the perforation datapoints are above it.

Figures 5 and 6 confirm the ability of the modified NNO BLE to predict the P/NP response of foam-filled dual wall systems more correctly, but now also at velocities as high as 30 km/s. In these figures, the P/NP datapoints are not always where they might be expected to be found with respect to their placement about the original NNO BLE. In Figure 5, e.g., most of the NP points are above the plot of the original NNO BLE (whereas they should be below it), and in Figure 6, most of the P datapoints are below it, whereas they should be above it.

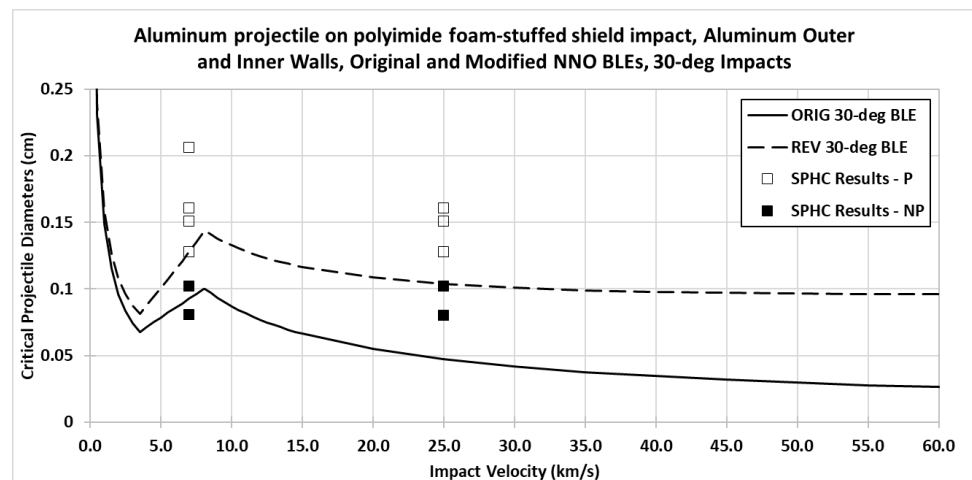


Figure 5. Comparison of Original and Modified NNO BLEs against P/NP data in [12] for Dual-Wall Systems with Aluminum Outer and Inner Walls.

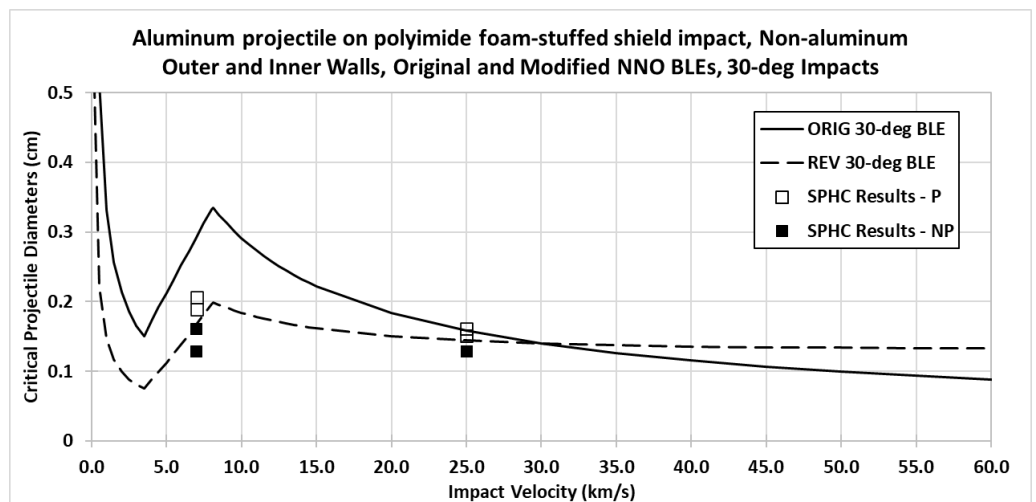


Figure 6. Comparison of Original and Modified NNO BLEs against P/NP data in [12] for Dual-Wall Systems with Non-Aluminum Outer and Inner Walls.

However, when the placements of the P/NP datapoints are compared against the plots of the modified NNO BLEs for these wall systems, we see that these points are now, for the most part, where they need to be. That is, the solid NP points in Figure 5 are now below the BLE curve, and in Figure 6, the hollow P points are now above it.

It is important to note that the comparisons shown in Figures 2–6 are those where the modified BLE is plotted against the datapoints used in the development of the modifications given by Equations (1)–(6). It would be instructive, of course, to compare the predictions of the original and modified NNO BLEs against some P/NP data from tests using targets that were not part of the dataset that was used in the development of those modifications. These comparisons are shown in Figures 7 and 8 below.

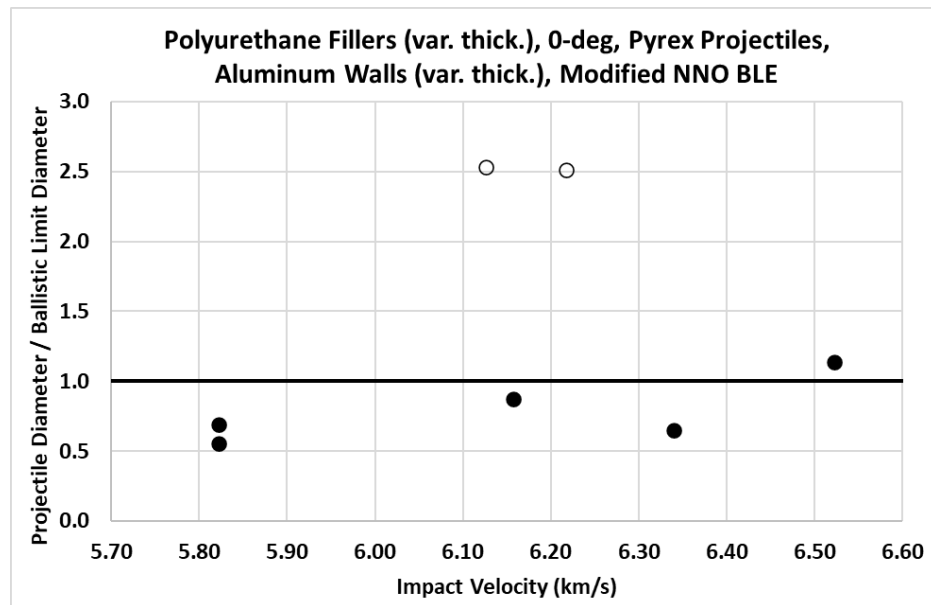


Figure 7. Comparison of Original and Modified NNO BLEs against P/NP data in [4,6] for Dual-Wall Systems with Aluminum Walls and a Polyurethane Filler.

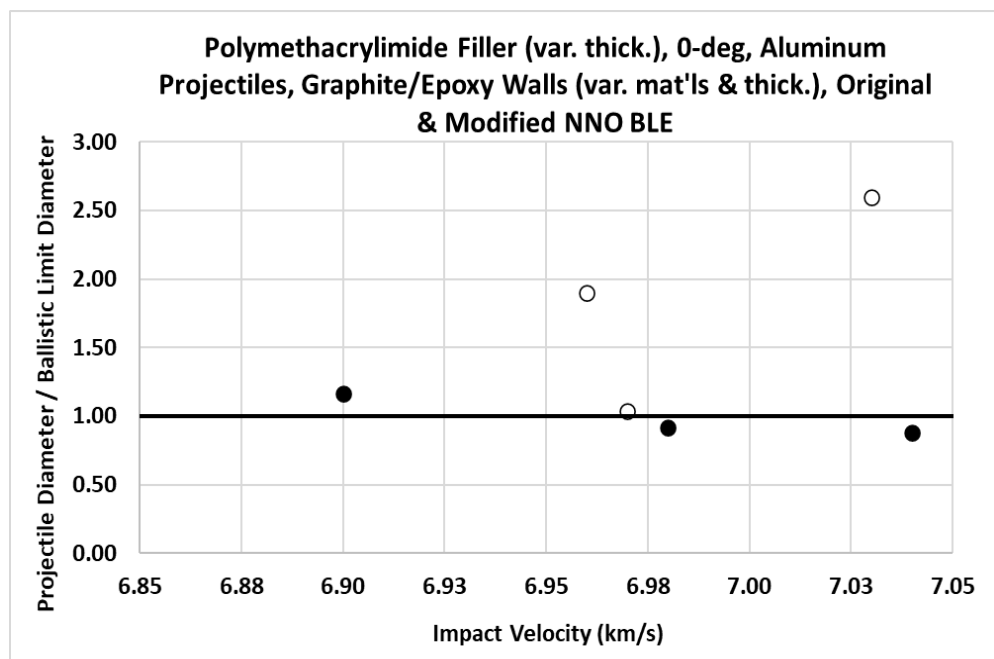


Figure 8. Comparison of Original and Modified NNO BLEs against P/NP data in [10,11] for Dual-Wall Systems with Non-Aluminum Walls and a Polymethacrylimide Filler.

In Figures 7 and 8 it is evident that the modified NNO BLE fared very well in predicting the P/NP response of the dual-wall systems and fillers under consideration. There was, of course, in each figure, one non-perforation datapoint that appeared on the side opposite to where it was expected. However, that kind of “spillage” is not at all surprising or unexpected (see, e.g., [15]).

Table 5 below presents a top-level overview of the ability of the original and modified NNO BLEs to correctly predict the P/NP response of a foam-filled dual-wall system. As can be seen in this table, there is a marked reduction in the number of incorrect response predictions (and a corresponding increase in the number of correct predictions) of the modified NNO BLE as compared to the original NNO BLE formulation. That is, in approx.

37% of the impact tests, the original NNO BLE incorrectly predicted whether or not the inner wall would be perforated. This occurred in only approx. 17% of the tests when the modified NNO BLE was used.

Table 5. Overview of Original and Modified NNO BLE Performance.

	Original NNO BLE		Modified NNO BLE	
P predicted as P	40	45%	42	47%
P predicted as NP	4	4%	1	1%
NP predicted as P	29	33%	14	16%
NP predicted as NP	16	18%	32	36%

As a final comment, we recall that the original formulation of the NNO BLE has three sections: a downward curving low velocity section, and upward sloping intermediate section, and a second less steep downward sloping high velocity section. In an effort to reduce the complexity of the modifications, the same modification formulation was applied to all three sections of the dual-wall BLE. The less-than-hoped for improvements to the NNO BLE when the modifications presented herein in the low and intermediate velocity sections seen in Figures 2, 3, 7 and 8 indicate that perhaps it might be necessary to investigate the possibility that the different sections of the dual-wall BLE might each need its own modification factor.

Similarly, the results in Figure 3 show that the predictions of the modified model at 0° are not as good as those at 30° as shown in Figures 5 and 6. The modification factor f_3 as given by Eq 6 does have an impact obliquity term. However, it might be necessary to explore the possibility of adding additional obliquity terms to the equations for modifications f_1 and f_2 to improve the agreement between experimental results and the modified NNO BLE, especially for 0-deg impacts.

5. Summary and Conclusions

A study was performed in which a frequently used BLE for dual-wall configurations that are commonly used on spacecraft to protect them against the MMOD environment was modified to more properly include the effects of any stuffing between the walls as well as the actual material properties of the walls and the impacting projectile. By comparing the predictions for ballistic limit diameter of the modified and original versions of this BLE, we found that there was, overall, a marked improvement in the response prediction ability once the modifications were introduced into the NNO BLE. This improvement was also evident when comparing original and modified NNO BLE predictions against empirical response data that were not used in developing these modifications. Using this modified version of the NNO BLE for these kinds of dual-wall systems will result in assessed mission risk values that would be more reflective of the actual spacecraft wall designs being used.

Funding: This research was supported by funding from the NASA Engineering Safety Center.

Informed Consent Statement: Not applicable.

Data Availability Statement: The data used in this study are wholly available in this article.

Acknowledgments: The author wishes to acknowledge the support provided by the NASA Engineering Safety Center that made this study possible. The author is also grateful to Joel Williamsen, Bob Stellingwerf, and Steve Evans for performing the hydrocode simulations that were used in this study, and to Eric Christiansen and the NASA team that performed the recent tests that were part of this study.

Conflicts of Interest: The author declares no conflict of interest.

References

1. Schonberg, W.P. Concise History of Ballistic Limit Equations for Multi-Wall Spacecraft Shielding. *Rev. Hum. Space Explor.* **2016**, *1*, 46–54. [[CrossRef](#)]
2. Christiansen, E.L. Design and Performance Equations for Advanced Meteoroid and Debris Shields. *Int. J. Impact Eng.* **1993**, *14*, 145–156. [[CrossRef](#)]
3. Material Property Data. Available online: <https://matweb.com/> (accessed on 27 December 2022).
4. Pipitone, S.J.; Reynolds, B.W. Effectiveness of Foam Structures for Meteoroid Protection. *J. Spacecr.* **1964**, *1*, 37–43. [[CrossRef](#)]
5. Lundeberg, J.F.; Stern, P.H.; Bristow, R.J. *Meteoroid Protection for Spacecraft Structures*; NASA CR-554201; NASA: Washington, DC, USA, October 1965.
6. Lundeberg, J.F.; Lee, D.H.; Burch, G.T. Impact Penetration of Manned Space Stations. *J. Spacecr.* **1966**, *3*, 182–186. [[CrossRef](#)]
7. Williams, J.G. *High-Velocity-Impact Tests Conducted with Polyethylene Terephthalate Projectiles and Flexible Composite Wall Panels*; NASA TN-D-6135; NASA: Washington, DC, USA, March 1971.
8. Hofmann, D.; Christiansen, E.; Lear, D.; Vander Kam, J.; Davis, B. *MSR MMG Debris Cloud HVI Study, Version 2*; NASA Johnson Space Center: Houston, TX, USA, 8 August 2021.
9. Sarli, B.V.; Christiansen, E.; Hofmann, D.; Lear, D.; Vander Kam, J.; Davis, B. *MSR-EEV MMG HVI Test Program, Version 10*; NASA Johnson Space Center: Houston, TX, USA, 17 October 2021.
10. Sarli, B.V.; Christiansen, E.; Hofmann, D.; Lear, D.; Squire, M.; Davis, B. *Enhanced Whipple Shield HVI Study, Version 7*; NASA Johnson Space Center: Houston, TX, USA, 3 March 2022.
11. Sarli, B.V.; Christiansen, E.; Needels, N.; Lear, D.; Stein, R.; Davis, B. *MSR-EEV MMG Shield Evaluation HVI Test Program, Version 14*; NASA Johnson Space Center: Houston, TX, USA, 28 September 2022.
12. Williamsen, J.; Stellingwerf, R.; Evans, S.; Squire, M. Prediction and Enhancement of Thermal Protection Systems from Meteoroid Damage Using a Smooth Particle Hydrodynamic Code. In Proceedings of the 2022 Hypervelocity Impact Symposium, Alexandria, VA, USA, 18–22 September 2022.
13. Rodrigues, R.; Figueiredo, L.; Diogo, H.; Bordado, J. Mechanical Behavior of PET Fibers and Textiles for Stent-Grafts Using Video Extensometry and Image Analysis. *Sci. Technol. Mater.* **2018**, *30*, 23–33. [[CrossRef](#)]
14. Rahman, M.; Ayatullah Hosne Asif, A.K.M.; Sarker, P.; Sarker, B. Improvement of Tensile Strength of Viscose Woven Fabric by Applying Chemical Finishes. *Manuf. Sci. Technol.* **2019**, *6*, 23–30. [[CrossRef](#)]
15. Schonberg, W.P.; Compton, L.E. Application of the NASA/JSC Whipple Shield Ballistic Limit Equations to Dual-Wall Targets under Hypervelocity Impact. *Int. J. Impact Eng.* **2008**, *35*, 1792–1798. [[CrossRef](#)]

Disclaimer/Publisher’s Note: The statements, opinions and data contained in all publications are solely those of the individual author(s) and contributor(s) and not of MDPI and/or the editor(s). MDPI and/or the editor(s) disclaim responsibility for any injury to people or property resulting from any ideas, methods, instructions or products referred to in the content.